OPEN

Experimental & Molecular Medicine (2018) 50, e422; doi:10.1038/emm.2017.175
Official journal of the Korean Society for Biochemistry and Molecular Biology
www.nature.com/emm

ORIGINAL ARTICLE

Depletion of S100A4$^+$ stromal cells does not prevent HCC development but reduces the stem cell-like phenotype of the tumors

Jingjing Jiao[1], Álvaro González[1], Heather L Stevenson[2], Mihai Gagea[3], Hikaru Sugimoto[4], Raghu Kalluri[4] and Laura Beretta[1]

There is a pressing need for the development of novel approaches to treat and prevent hepatocellular carcinoma (HCC). The S100 calcium-binding protein S100A4 is associated with poor prognosis and metastasis in several human cancers. In addition, a role for S100A4 in modulating cancer-initiating cells stemness properties was recently proposed in head and neck and gastric cancers. Whether S100A4$^+$ stromal cells contribute to tumor onset remains, however, an unanswered question. To address that question, we generated a new mouse model allowing for the depletion of S100A4$^+$ cells in a mouse model of HCC with stemness properties, by crossing mice with hepatic deletion of phosphatase and tensin homolog (PTEN) with mice expressing viral thymidine kinase under the control of S100A4 promoter. Depletion of S100A4$^+$ cells by ganciclovir injection did not prevent the development of HCC but reduced the stemness phenotype of the tumor as measured by the expression of progenitor cell, biliary cell and hepatocyte markers. The results were further confirmed by histology analysis showing reduction of cholangiolar tumor components and degree of oval cell hyperplasia in the adjacent liver. Depletion of S100A4$^+$ cells had also some beneficial effect on the underlying liver disease with a reduction of NAS score, largely due to the reduction of inflammation. In conclusion, this study demonstrated that S100A4$^+$ cells do not contribute to HCC onset but maintain the stemness phenotype of the tumor. This study also suggests for the first time a crosstalk between inflammation and stemness.
Experimental & Molecular Medicine (2018) **50,** e422; doi:10.1038/emm.2017.175; published online 5 January 2018

INTRODUCTION

Hepatocellular carcinoma (HCC) is the second most common cause of cancer-related mortality worldwide.[1] Although the highest rates of liver cancer are found in certain areas of Asia and Africa, liver cancer incidence and mortality rates are increasing strikingly in western countries, including the United States.[2,3] Liver cirrhosis due to hepatitis B virus, hepatitis C virus, high alcohol consumption or non-alcoholic steatohepatitis is the main risk factor associated with HCC and most patients with HCC have compromised liver function, limiting treatment options.[4] Survival rates are low, remaining at 15% at 5 years. Thus, there is a pressing need for the development of novel approaches to treat and prevent HCC.[5]

The S100 calcium-binding protein A4 (S100A4) is a member of the S100 protein family.[6] Expression of S100A4 is associated with poor prognosis in several human cancers including breast and colorectal cancers.[7,8] S100A4 also has a role in promoting metastatis[9–11] and in epithelial-mesenchymal transition in colorectal cancer[12,13] and ovarian cancer.[14] In HCC, abnormal expression of S100A4 correlates with poor prognosis.[15] A role in metastasis and epithelial-mesenchymal transition for S100A4 was also proposed in HCC[16–19] as well as in cholangiocarcinoma.[20–22] Furthermore, S100A4 induced liver fibrosis and activation of hepatic stellate cells, suggesting that S100A4 could also be a marker for liver fibrogenesis and a target for novel antifibrotic strategies.[23,24]

The role of S100A4 in carcinogenesis, in hepatocarcinogenesis in particular, is unknown. In prior studies, we showed that in mice with hepatic deletion of *Pten*, anti-miR-21 treatment reduced liver tumor growth and prevented tumor development. These effects were accompanied with a decrease in liver fibrosis and a concomitant reduction of CD24$^+$ liver progenitor cells and S100A4$^+$ cancer-associated stromal cells.[25] To assess the role of S100A4$^+$ stromal cells in HCC onset, we crossed

[1]Department of Molecular and Cellular Oncology, The University of Texas MD Anderson Cancer Center, Houston, TX, USA; [2]Department of Pathology, University of Texas Medical Branch, Galveston, TX, USA; [3]Department of Veterinary Medicine & Surgery, The University of Texas MD Anderson Cancer Center, Houston, TX, USA and [4]Department of Cancer Biology, The University of Texas MD Anderson Cancer Center, Houston, TX, USA
Correspondence: Dr L Beretta, Department of Molecular and Cellular Oncology, The University of Texas MD Anderson Cancer Center, Rm S11.8336c 1515 Holcombe Boulevard, Houston, TX 77030, USA.
E-mail: lberetta@mdanderson.org
Received 21 April 2017; accepted 11 May 2017

mice with hepatic deletion of *Pten* and mice expressing viral thymidine kinase under the control of S100A4 promoter (*S100A4-tk* mice). In *S100A4-tk* mice, ganciclovir (GCV) treatment results in the selective ablation of $S100A4^+$ stromal cells.[26] Mice with hepatocytic-deletion of *Pten* develop liver disease marked by steatosis, inflammation and fibrosis characteristic of non-alcoholic steatohepatitis, which progresses to HCC with stemness properties.[25,27–30]

MATERIALS AND METHODS

Mice generation and treatment

Mouse studies were approved by the MDACC Institutional Animal Care and Use Committee. Liver-specific *Pten* knockout mice (*Pten* $^{loxP/loxP}$; *Alb-Cre*$^+$) were crossed with *S100A4-tk* mice (B6.Cg-Tg (S100a4-TK) M31Egn/YunkJ) to generate *Pten-S100A4* double transgenic mice. For this model, control animals were *Pten*$^{loxP/loxP}$; *Alb-Cre*$^+$; *S100A4-tk*$^-$ (referred as PTEN-TK$^-$) while the experimental mice were *Pten*$^{loxP/loxP}$; *Alb-Cre*$^+$; *S100A4-tk*$^+$ (referred as PTEN-TK$^+$). To deplete $S100A4^+$ cells, ganciclovir (GCV) was injected intraperitoneally (50 mg per kg of body weight in a final volume of 500 µl phosphate-buffered saline). Five rounds of treatment were given to mice, with each round consisting of one injection (50 mg kg^{-1}, i.p.) per day for 1 week, and 1 week of interval. In *Pten-S100A4* double transgenic mice, GCV treatment was initiated at 7-month-of age. For diethylnitrosamine (DEN) model, HCC was induced by the combination of 25 mg kg^{-1} DEN given at day 15 postpartum and 17 weekly injections of CCl_4 (0.5 ml kg^{-1} i.p., dissolved in corn oil) starting at 5-week of age.

Quantitative PCR

For quantitation of target gene expression levels, equal amounts of RNA samples were submitted to reverse transcription and real-time PCR using the following primers: HNF4A: F:5′-AGCTTGCC TTATAGTACTCCT-3′, R:5′-AGAGATGGCTTTAGAGAAGTC-3′; Albumin: F:5′-TACACTTCCTGAAGATCAGAG-3′, R:5′-AGAGAT GGCTTTAGAGAAGTC-3′; KRT19: F:5′-GAAGTCAGTATGA GATCATGG-3′, R:5′-GTCTTGCTTATCTGGATCTG-3′; OPN: F:5′-AGTACACAAGCAGACACTTTC-3′, R:5′-ATCAGGATACTGTTCAT CAGA-3′; S100A4: F:5′-CTGGGGAAAAGGACAGATGA-3′; R:5′-TGC AGGACAGGAAGACACAG-3′; CD24: F:5′-CCCGTACAGTAGTCTT GATAA-3′; R:5′-AATAGATGTACAGCATTCAGG-3′. PCR amplifications of the respective genes were performed with iTaq SYBR Green Supermix (Bio-Rad, Hercules, CA, USA) in CFX Connect Real-Time System (Bio-Rad). The Bio-Rad CFX Manager software (version 2.1) was used for calculation of threshold cycles (Ct)-values and melting curve analysis of amplified DNA. Relative expression of the genes was calculated by $2-TTCt$ method.

Histopathology analysis, tissue immunohistochemistry staining

Liver and tumor tissues were collected from mice at the time of necropsy. Immediately after euthanasia and gross examination, tissue samples were collected as snap-frozen in liquid nitrogen and fixed in 10% neutral buffered formalin. The snap-frozen tissues were ground for RNA extraction. The formalin fixed tissues were processed histologically, embedded in paraffin blocks, and cut in 4-µm-thick sections that were stained with hematoxylin and eosin, Masson's trichrome or immunohistochemistry. All lesions above 7.8 mm^3 detected at necropsy, were included for histology analysis. Hyperplastic and neoplastic lesions of liver were evaluated by a veterinary pathologist and classified according with the 'International Classification of Rodent Tumors—The Mouse' by Ulrich Mohr, 2001. In these mice, were detected hyperplastic lesions of hepatocytes, oval cells and bile ducts; neoplastic being tumors such as hepatocellular adenomas; and neoplastic malignant tumors including HCC, cholangiocarcinoma and hepatocholangiocellular carcinoma. No preneoplastic lesions of liver were described in these mice. For S100A4 immunohistochemistry staining, paraffin slides were deparaffinized and rehydrated. Antigen retrieval was performed by heating in Tris-EDTA buffer (10 mM Tris Base, 1 mM EDTA Solution, 0.05% Tween 20, pH 9.0). Sections were blocked in TAE buffer containing 10% bovine serum albumin and 0.03% Triton X-100 for 30 min and incubated with S100A4 (DAKO, Glostrup, Denmark, 1:100) overnight at 4°. Slides were washed in phosphate-buffered saline and incubated with horseradish peroxidase-conjugated goat anti rabbit secondary antibodies (DAKO) at dilution of 1:400 for 30 min at room temperature. S100A4-positive cell were visualized by DAB chromogen (Cell Signaling, Danvers, MA, USA). S100A4-positive staining area were quantified by Imagescope (Aperio, Vista, CA, USA).

Statistical analysis

Data are presented as mean ± s.e.m. Statistical difference between each group was assessed by unpaired Student *t*-test, which was assessed by χ^2-test using Graphpad 6.0 software (Graphpad software, San Diego, CA, USA). A value of $P<0.05$ was considered significant.

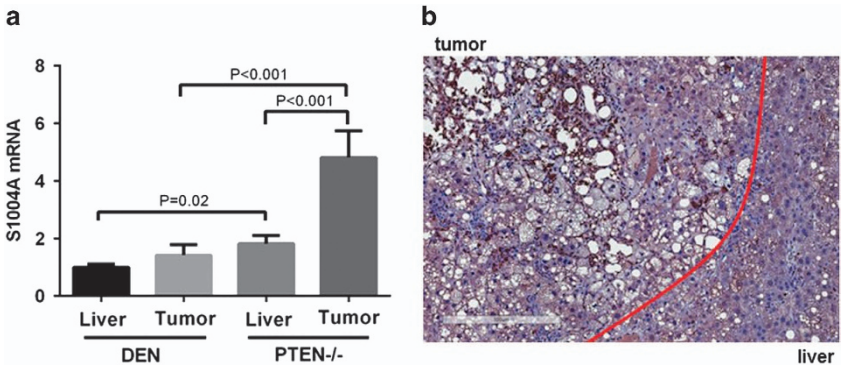

Figure 1 Expression of S100A4 in mouse models of liver cancer. (**a**) Expression of S100A4 was measured by quantitative PCR in liver and tumor of DEN model and PTEN−/− model. Data are shown as fold change and standard error of the mean (unpaired student *t*-test). (**b**) Immunohistochemistry staining of S100A4 on liver tumor sections from PTEN−/− mice. Scale bar, 300 µm.

RESULTS

S100A4 expression in liver and tumors in mouse models of HCC

We first measured S100A4 mRNA expression in liver and tumors of two mouse models of HCC: mice treated with a combination of diethylnitrosamine (DEN) and the hepatotoxin carbon tetrachloride (CCl_4) and mice with hepatocytic deletion of Pten. While HCCs in the DEN model are well differentiated, tumors in *Pten*−/− model present stemness properties with a mixture of cholangiocarcinomas and HCCs. In both liver and tumors, S100A4 expression was significant higher in *Pten*−/− model that in DEN model (1.82-fold; $P=0.02$ and 3.39-fold; $P<0.001$, respectively) (Figure 1a). Figure 1b shows representative expression of S100A4 and tumor and adjacent liver in *Pten*-null mice measured by immunohistochemistry staining. These results suggest that S100A4 expression correlates with stemness properties in HCC.

Generation of *Pten-S100A4* double transgenic mice

To assess the role of S100A4$^+$ cells in the development of liver cancer, we generated *Pten-S100A4* double transgenic mice that were derived from crossing *S100A4-tk* mice with liver-specific *Pten*−/− mice. In this new model, S100A4$^+$ cells can be depleted by administration of ganciclovir. Mice negative for TK gene were also treated with ganciclovir as controls. We first evaluated whether ganciclovir treatment reduced S100A4$^+$ cell populations by quantification of S100A4 immunohistochemistry staining. Ganciclovir injection led to a 57% decrease of S100A4 in the liver ($P<0.001$) (Figure 2a) and to a 50% decrease in tumors ($P<0.001$) (Figure 2b). Representative images are shown in Figure 2.

S100A4$^+$ stromal cells depletion did not prevent HCC development

As shown in Figure 3, in controls PTEN-TK$^-$ mice that do not respond to ganciclovir treatment, 100% of mice had tumors at 9 months of age while 83.3% of the PTEN-TK$^+$ mice, treated with ganciclovir and therefore depleted of S100A4$^+$ cells, had tumors (Figure 3a). Depletion of S100A4$^+$ cells led to a decrease in average tumor volume from 48.89 to 28.89 mm^3, but this effect was not statistically significant (Figure 3b). The average number of tumors per mouse in PTEN-TK$^-$ and PTEN-TK$^+$ was similar (2.2 vs 2.0, respectively) (Figure 3c).

S100A4$^+$ cells depletion abolished the biliary type tumor in *Pten*-null mice

Interestingly, we observed a tumor type change in PTEN-TK$^+$ group after S100A4$^+$ cells depletion as evaluated by histopathological analysis. In control PTEN-TK$^-$ group, 37% of the tumors were HCCs, 45% were hepatocellular adenomas, 9% were cholangiocarcinomas and 9% were hepatocholangiocellular carcinomas. No biliary tumor phenotypes were observed in PTEN-TK$^+$ mice (Figure 4a). Representative histology images of each tumor type are shown in Figure 4b.

S100A4$^+$ cells depletion reduced oval cell hyperplasia in *Pten*-null mice

In agreement with the inhibition of biliary tumor components in PTEN-TK$^+$ mice after S100A4$^+$ cells depletion, a decrease in the degree of oval cell hyperplasia was also observed. Only 8.3% of the PTEN-TK$^+$ liver had moderate to marked degrees of oval cell hyperplasia (scores 3–4) while 35.3% of the control PTEN-TK$^-$ liver had oval cell hyperplasia with scores 3–4 ($P=0.04$) (Figure 5a). Representative images are shown in Figure 5c. The control PTEN-TK$^-$ group also had higher percentage of high degree of bile duct hyperplasia (23.5 vs 8.3%), but these changes did not reach significance (Figure 5b).

S100A4$^+$ depletion inhibited non-alcoholic steatohepatitis and inflammation

Histological analysis also showed a mild but significant decrease in non-alcoholic steatohepatitis severity as reflected by non-alcoholic fatty liver disease activity scores (NAS) ($P=0.03$). This effect was largely due to a decrease in inflammation ($P=0.02$) in PTEN-TK$^+$ liver (Figures 6a and e). No significant effect was observed on other liver histology parameters such as degenerative ballooning, steatosis or fibrosis (Figures 6b–d and f).

S100A4$^+$ cells depletion correlated with reduction of stemness and increased hepatocytic differentiation

We measured the expression of progenitor cell, biliary cell and hepatocyte markers after S100A4$^+$ cell depletion. Expression of progenitor cell marker osteopontin (OPN) and CD24 was significantly decreased in PTEN-TK$^+$ liver (−2.7-fold, $P<0.001$ and −2.1-fold, $P=0.006$, respectively) and tumor (−1.8-fold, $P<0.001$ and −1.9-fold $P=0.03$ respectively). Expression of biliary cell marker Keratin 19 (KRT19) was also significantly decreased in PTEN-TK$^+$ tumor (−2.6-fold, $P=0.04$) (Figures 7a–c). In contrast, the expression of hepatocyte markers Hepatocyte Nuclear Factor 4 Alpha (HNF4A) and albumin was increased in PTEN-TK$^+$ tumors (1.4- fold, $P=0.003$ and 2.0-fold, $P=0.01$, respectively) (Figures 7d and e).

DISCUSSION

In the United States, deaths from liver cancer increased at the highest rate of all cancer sites.[3] Survival has not significantly improved in decades and the current 5-year survival rate is only 17.5%. HCCs with mixed HCC/cholangiocarcinoma phenotype and those with stemness properties have a worse prognosis and higher risk of recurrence. The large majority of HCC cases are diagnosed at a late stage and a challenge in the clinical care of HCC patients is that over 90% of patients with HCC have underlying liver cirrhosis and compromised liver function, limiting treatment options. Treatment of HCC remains a huge unmet need.

Cancer stem cells have the ability to self-renew, differentiate and proliferate, have greater tumorigenicity and chemoresistance, and have been associated with a poor prognosis in several human malignancies.[31] Targeting the regulatory mechanism of their self-renewal and differentiation capacity

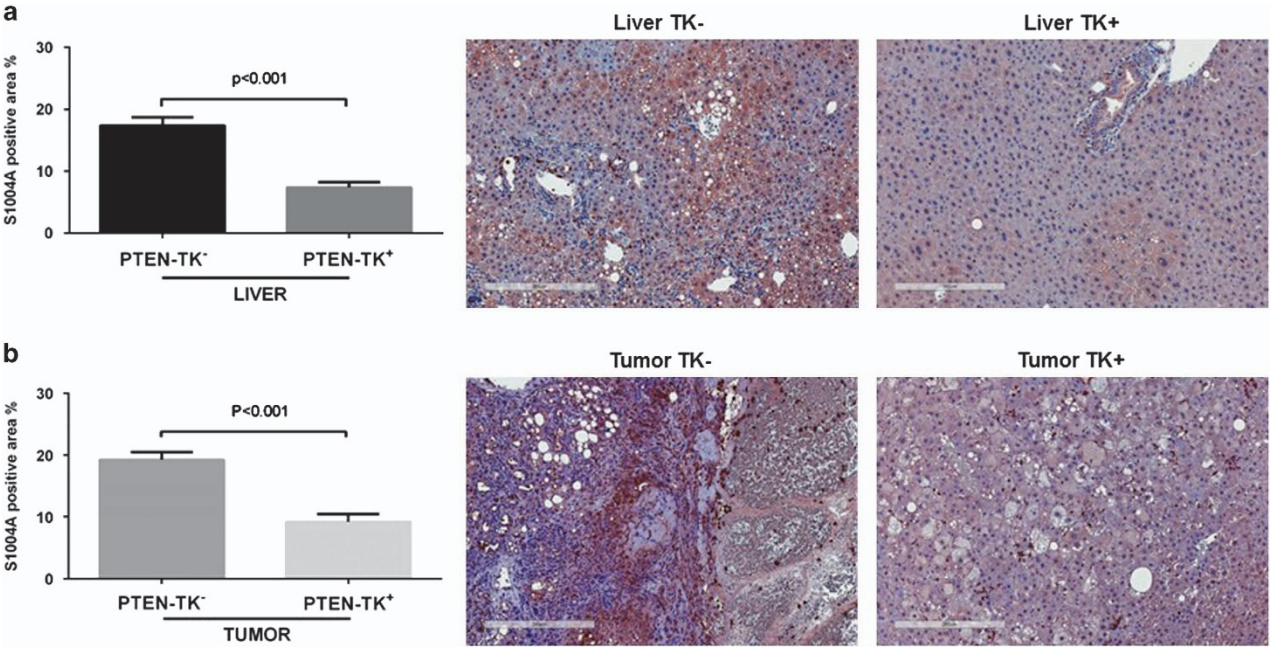

Figure 2 Depletion of S100A4-positive cells in the liver and the tumor. Reduction of S100A4-positive cells in TK+ mice shown with quantification data calculated using the percentage of positive staining areas and representative immunohistochemistry staining of S100A4 in both liver (**a**) and tumor (**b**). Scale bar, 300 μm.

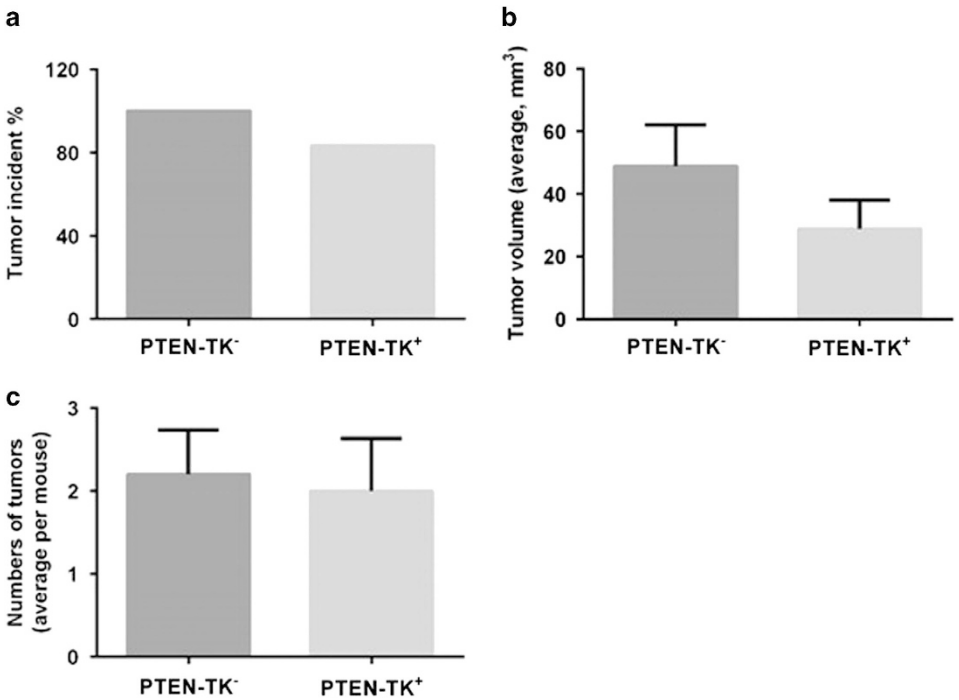

Figure 3 Effect of S100A4 cell depletion on tumor prevention *in vivo*. Graphs showing effect of S100A4 depletion on tumor incidence (**a**), average tumor volume per mouse (**b**) and average number of tumors per mouse (**c**). Tumor sizes were measured with calipers in three dimensions at necropsy. Tumor volumes were calculated using the formula tumor volume (mm^3) = ($L \times W^2$)/2, where L is length and W is width. Graphs were shown as mean ± s.e.m.

is a promising strategy for both therapy and chemoprevention. Our group recently reported that the induction of hepatocyte differentiation by miR-148a treatment reduces HCC tumor growth and prevents tumor development in mice with hepatic deletion of *Pten*.[30] We also reported that anti-miR-21 treatment of *Pten*-null mice, reduces liver tumor growth and prevents

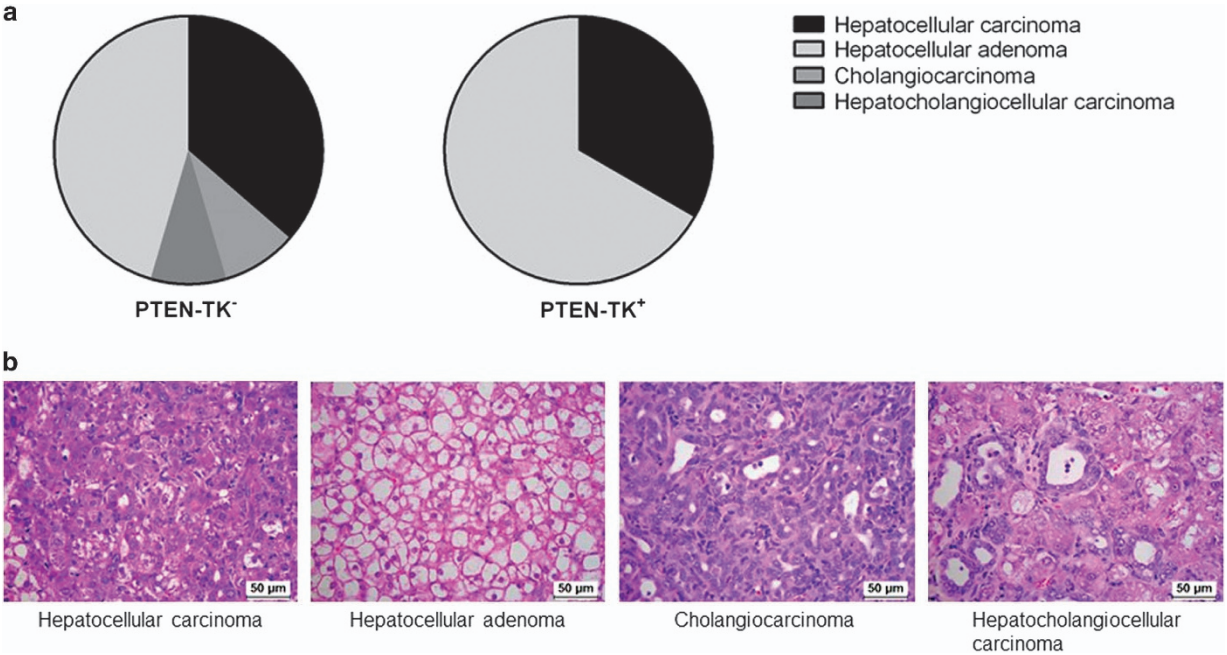

Figure 4 Effect of S100A4 cell depletion on tumor type. (**a**) Pie charts represented the overall tumor histology distribution in PTEN-TK$^+$ and PTEN-TK$^-$ mice. (**b**) Representative histology images of each tumor type. Scale bar, 50 μm

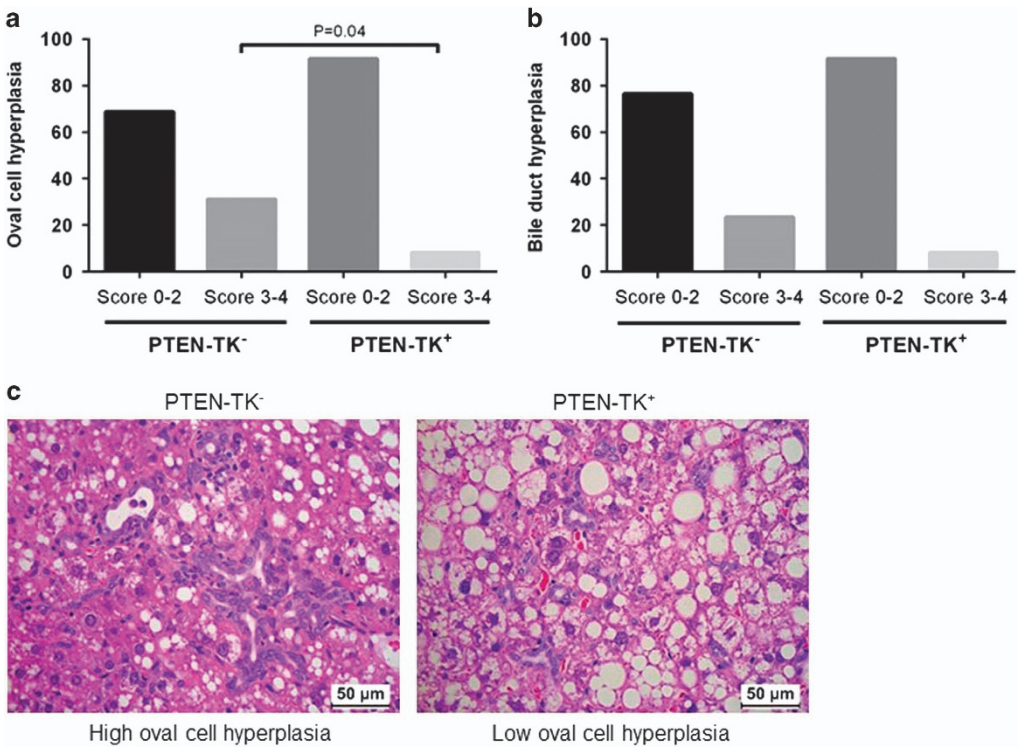

Figure 5 Effect of S100A4 cell depletion on hepatic oval cell hyperplasia (**a**) and bile duct hyperplasia (**b**). Both were accessed on 1 to 4 scale, score 0 for no lesion, 1 for lesion affects less than 10% of the tissue, 2 for lesion affects 10–20% of the tissue, 3 for lesion affects 20–40% of the tissue and 4 for lesion affects 40–100% of the tissue. (**c**) Representative images showing hepatic oval cell hyperplasia in PTEN-TK$^-$ and PTEN-TK$^+$ mice.

tumor development, effects accompanied with a decrease in liver fibrosis and a concomitant reduction of CD24$^+$ liver progenitor cells and S100A4$^+$ cancer-associated stromal cells.[25]

S100A4$^+$ cells likely represent an heterogeneous cell population, including cancer-associated fibroblasts and inflammatory macrophages.[32,33] The role of each S100A4$^+$ cell subpopulation in the crosstalk between S100A4$^+$ cells and cancer stem cells

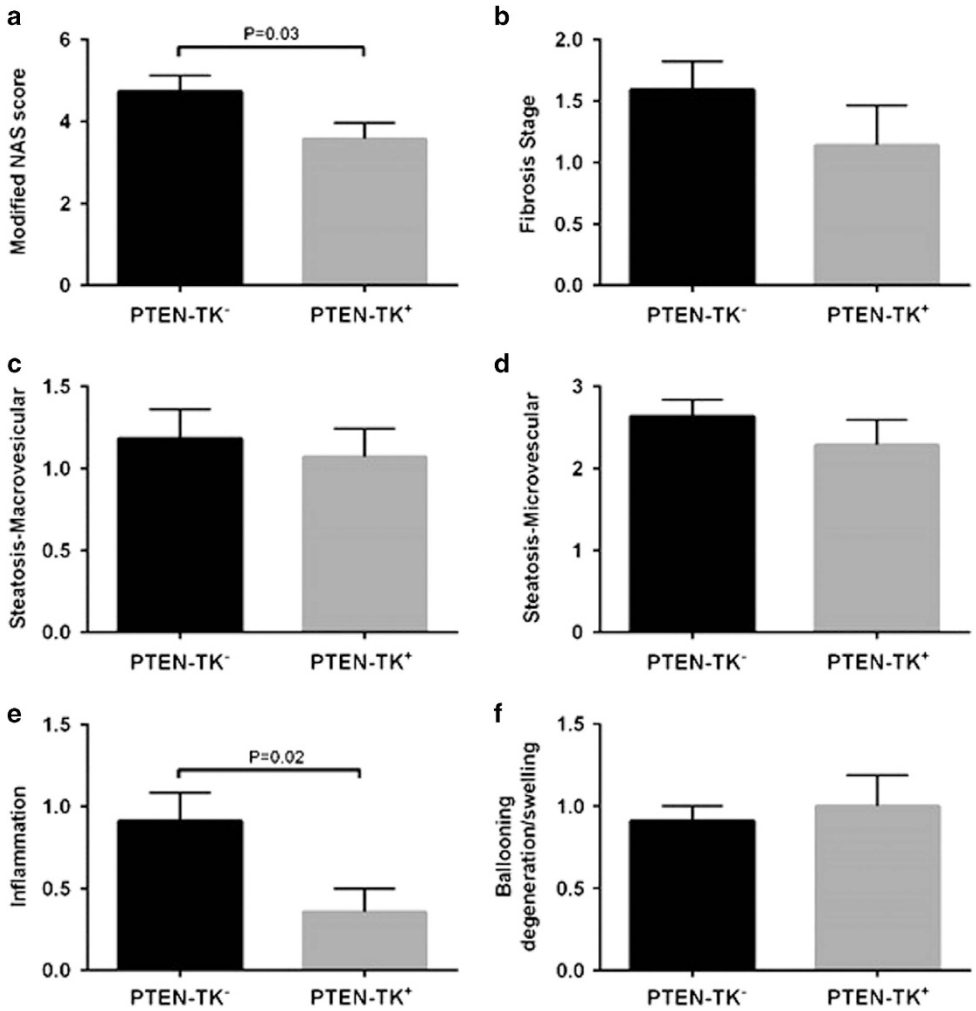

Figure 6 Effect of S100A4 cell depletion on hepatic histopathology. (**a**) Modified NAS is the Sum of marcrosteatosis, microsteatosis, inflammation and ballooning scores. (**b**) Liver fibrosis stage was individually scored as 0 for no fibrosis, 1 for periportal or perivenular fibrosis, 2 for periportal and perivenular, 3 for bridging fibrosis and 4 for cirrhosis. (**c**, **d**) Steatosis was individually scored by macrosteatosis (**c**) and microsteatosis (**d**) (0 for $<5\%$, 1 for 5–33%, 2 for 33–66%, and 3 for more than 66%). (**e**) Inflammation was graded by overall assessment of all inflammatory foci (0 for no foci, 1 for <2, 2 for 2–4 foci, and 3 for >4 foci). (**f**) Ballooning score was 0 for no ballooned cells per field, 1 for few, and 2 for many.

remain to be determined. The contribution of S100A4 in modulating cancer-initiating cells stemness properties was first proposed in head and neck and gastric cancers.[34,35] A role for S100A4 in tumor onset in intestinal tumors was also investigated using genetic ablation or overexpression.[36] That later study concluded that S100A4 does not affect tumor initiation in the intestinal tract but confirmed the role of S100A4 in tumor metastasis. Therefore, the role of S100A4 and S100A4$^+$ cells in tumor onset remains an important unanswered question. To address that question, we generated a new mouse model allowing for the depletion of S100A4$^+$ in a mouse model of HCC with stemness properties. Our data showed that although depleting S100A4$^+$ cells did not prevent the development of HCC, it reduced the stemness of the tumor as measured by the expression of progenitor cell markers CD24 and osteopontin and biliary marker KRT19. The results were further confirmed by histology analysis showing reduction of cholangiolar tumor components and of the degree of oval cell hyperplasia in the adjacent liver. In contrast, hepatocyte markers albumin and HNF4A were upregulated upon the depletion of S100A4 expressing cells, supporting a role of S100A4 expressing cells in differentiation and progenitor cells survival. This is particularly relevant considering our recent demonstration that differentiation-targeted therapy is a promising approach for the treatment of HCC.[30]

Besides the effects on tumor, our data showed that depletion of S100A4$^+$ cells has some beneficial effect on the underlying liver disease with a reduction of NAS scores, largely due to the reduction of inflammation. The involvement of S100A4 in chronic inflammation was previously demonstrated in conditions such as rheumatoid arthritis[37] and myositis.[38] However, we did not observe any reduction of fibrosis.

In conclusion, this study demonstrated that S100A4$^+$ cells do not contribute to HCC onset but maintain the stemness

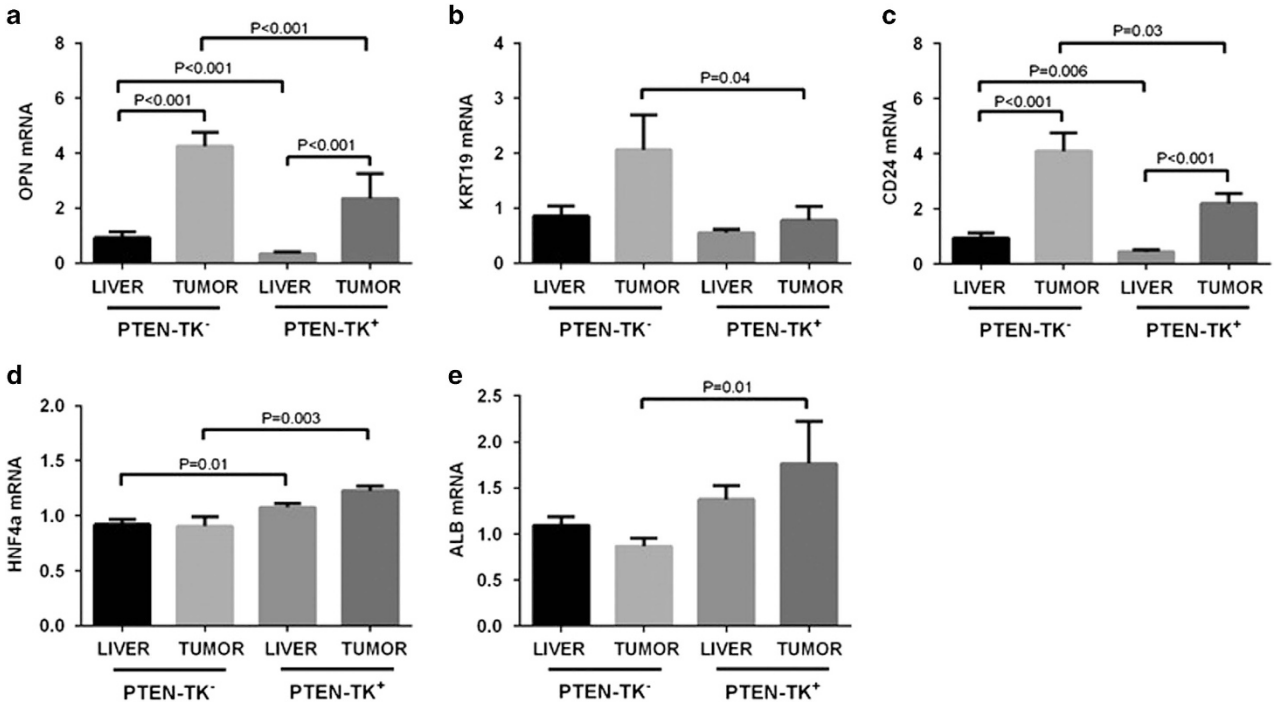

Figure 7 S100A4 cell depletion reduced stem-like phenotype and promoted hepatocytic differentiation phenotype. (**a**–**e**) Expression of progenitor markers osteopontin and CD24, biliary cell markers KRT19, and hepatocyte markers HNF4A and albumin was measured by quantitative PCR in tumors and livers of PTEN-TK$^+$ and PTEN-TK$^-$ mice. Results shown as mean ± s.e.m. (unpaired Student *t*-test).

phenotype of the tumor. This study also suggests for the first time a crosstalk between inflammation and stemness.

CONFLICT OF INTEREST

The authors declare no conflict of interest.

ACKNOWLEDGEMENTS

We thank Hong Shen for assistance in animal experiments. This work was supported by UTHealth Innovation for Cancer Prevention Research Training Program Post-doctoral Fellowship (Cancer Prevention and Research Institute of Texas grant # RP160015), by the National Institutes of Health through Cancer Center Support grant P30CA016672 and grant CA125550.

PUBLISHER'S NOTE

1 Jemal A, Bray F, Center MM, Ferlay J, Ward E, Forman D. Global cancer statistics. *CA Cancer J Clin* 2011; **61**: 69–90.
2 El-Serag HB. Hepatocellular carcinoma: recent trends in the United States. *Gastroenterology* 2004; **127**: S27–S34.
3 Ryerson AB, Eheman CR, Altekruse SF, Ward JW, Jemal A, Sherman RL *et al.* Annual Report to the Nation on the Status of Cancer, 1975-2012, featuring the increasing incidence of liver cancer. *Cancer* 2016; **122**: 1312–1337.
4 Bruix J, Sherman M. Management of hepatocellular carcinoma: an update. *Hepatology* 2011; **53**: 1020–1022.
5 Kim H, Park YN. Hepatocellular carcinomas expressing 'stemness'-related markers: clinicopathological characteristics. *Dig Dis* 2014; **32**: 778–785.
6 Helfman DM, Kim EJ, Lukanidin E, Grigorian M. The metastasis associated protein S100A4: role in tumour progression and metastasis. *Br J Cancer* 2005; **92**: 1955–1958.
7 Egeland EV, Boye K, Park D, Synnestvedt M, Sauer T, Oslo Breast Cancer C *et al.* Prognostic significance of S100A4-expression and subcellular localization in early-stage breast cancer. *Breast Cancer Res Treat* 2017; **162**: 127–137.
8 Boye K, Jacob H, Frikstad KA, Nesland JM, Maelandsmo GM, Dahl O *et al.* Prognostic significance of S100A4 expression in stage II and III colorectal cancer: results from a population-based series and a randomized phase III study on adjuvant chemotherapy. *Cancer Med* 2016; **5**: 1840–1849.
9 Ismail TM, Bennett D, Platt-Higgins AM, Al-Medhity M, Barraclough R, Rudland PS. S100A4 elevation empowers expression of metastasis effector molecules in human breast cancer. *Cancer Res* 2017; **77**: 780–789.
10 Dahlmann M, Kobelt D, Walther W, Mudduluru G, Stein U. S100A4 in cancer metastasis: Wnt signaling-driven interventions for metastasis restriction. *Cancers* 2016; **8**: 59.
11 Stewart RL, Carpenter BL, West DS, Knifley T, Liu L, Wang C *et al.* S100A4 drives non-small cell lung cancer invasion, associates with poor prognosis, and is effectively targeted by the FDA-approved anti-helminthic agent niclosamide. *Oncotarget* 2016; **7**: 34630–34642.
12 He Z, Yu L, Luo S, Li M, Li J, Li Q *et al.* miR-296 inhibits the metastasis and epithelial-mesenchymal transition of colorectal cancer by targeting S100A4. *BMC Cancer* 2017; **17**: 140.
13 Gomez-Contreras P, Ramiro-Diaz JM, Sierra A, Stipp C, Domann FE, Weigel RJ *et al.* Extracellular matrix 1 (ECM1) regulates the actin cytoskeletal architecture of aggressive breast cancer cells in part via S100A4 and Rho-family GTPases. *Clin Exp Metastasis* 2017; **34**: 37–49.
14 Yan W, Chen J, Chen Z, Chen H. Deregulated miR-296/S100A4 axis promotes tumor invasion by inducing epithelial-mesenchymal transition in human ovarian cancer. *Am J Cancer Res* 2016; **6**: 260–269.
15 Zhai X, Zhu H, Wang W, Zhang S, Zhang Y, Mao G. Abnormal expression of EMT-related proteins, S100A4, vimentin and E-cadherin, is correlated with clinicopathological features and prognosis in HCC. *Med Oncol* 2014; **31**: 970.
16 Dou C, Liu Z, Xu M, Jia Y, Wang Y, Li Q *et al.* miR-187-3p inhibits the metastasis and epithelial-mesenchymal transition of hepatocellular carcinoma by targeting S100A4. *Cancer Lett* 2016; **381**: 380–390.

17 Cadamuro M, Spagnuolo G, Sambado L, Indraccolo S, Nardo G, Rosato A *et al.* Low-dose paclitaxel reduces S100A4 nuclear import to inhibit invasion and hematogenous metastasis of cholangiocarcinoma. *Cancer Res* 2016; **76**: 4775–4784.
18 Yan XL, Jia YL, Chen L, Zeng Q, Zhou JN, Fu CJ *et al.* Hepatocellular carcinoma-associated mesenchymal stem cells promote hepatocarcinoma progression: role of the S100A4-miR155-SOCS1-MMP9 axis. *Hepatology* 2013; **57**: 2274–2286.
19 Cui JF, Liu YK, Zhang LJ, Shen HL, Song HY, Dai Z *et al.* Identification of metastasis candidate proteins among HCC cell lines by comparative proteome and biological function analysis of S100A4 in metastasis *in vitro*. *Proteomics* 2006; **6**: 5953–5961.
20 Techasen A, Namwat N, Loilome W, Duangkumpha K, Puapairoj A, Saya H *et al.* Tumor necrosis factor-alpha modulates epithelial mesenchymal transition mediators ZEB2 and S100A4 to promote cholangiocarcinoma progression. *J Hepatobiliary Pancreat Sci* 2014; **21**: 703–711.
21 Tian X, Wang Q, Li Y, Hu J, Wu L, Ding Q *et al.* The expression of S100A4 protein in human intrahepatic cholangiocarcinoma: clinicopathologic significance and prognostic value. *Pathol Oncol Res* 2015; **21**: 195–201.
22 Sato Y, Harada K, Sasaki M, Nakanuma Y. Clinicopathological significance of S100 protein expression in cholangiocarcinoma. *J Gastroenterol Hepatol* 2013; **28**: 1422–1429.
23 Chen L, Li J, Zhang J, Dai C, Liu X, Wang J *et al.* S100A4 promotes liver fibrosis via activation of hepatic stellate cells. *J Hepatol* 2015; **62**: 156–164.
24 Louka ML, Ramzy MM. Involvement of fibroblast-specific protein 1 (S100A4) and matrix metalloproteinase-13 (MMP-13) in CCl4-induced reversible liver fibrosis. *Gene* 2016; **579**: 29–33.
25 Zhang J, Jiao J, Cermelli S, Muir K, Jung KH, Zou R *et al.* miR-21 inhibition reduces liver fibrosis and prevents tumor development by inducing apoptosis of CD24+ progenitor cells. *Cancer Res* 2015; **75**: 1859–1867.
26 O'Connell JT, Sugimoto H, Cooke VG, MacDonald BA, Mehta AI, LeBleu VS *et al.* VEGF-A and Tenascin-C produced by S100A4^{+} stromal cells are important for metastatic colonization. *Proc Natl Acad Sci USA* 2011; **108**: 16002–16007.
27 Horie Y, Suzuki A, Kataoka E, Sasaki T, Hamada K, Sasaki J *et al.* Hepatocyte-specific Pten deficiency results in steatohepatitis and hepatocellular carcinomas. *J Clin Invest* 2004; **113**: 1774–1783.
28 Stiles B, Wang Y, Stahl A, Bassilian S, Lee WP, Kim YJ *et al.* Liver-specific deletion of negative regulator Pten results in fatty liver and insulin hypersensitivity [corrected]. *Proc Natl Acad Sci USA* 2004; **101**: 2082–2087.
29 Lai KK, Shang S, Lohia N, Booth GC, Masse DJ, Fausto N *et al.* Extracellular matrix dynamics in hepatocarcinogenesis: a comparative proteomics study of PDGFC transgenic and Pten null mouse models. *PLoS Genet* 2011; **7**: e1002147.
30 Jung KH, Zhang J, Zhou C, Shen H, Gagea M, Rodriguez-Aguayo C *et al.* Differentiation therapy for hepatocellular carcinoma: multifaceted effects of miR-148a on tumor growth and phenotype and liver fibrosis. *Hepatology* 2016; **63**: 864–879.
31 Visvader JE, Lindeman GJ. Cancer stem cells in solid tumours: accumulating evidence and unresolved questions. *Nat Rev Cancer* 2008; **8**: 755–768.
32 Sugimoto H, Mundel TM, Kieran MW, Kalluri R. Identification of fibroblast heterogeneity in the tumor microenvironment. *Cancer Biol Ther* 2006; **5**: 1640–1646.
33 Osterreicher CH, Penz-Osterreicher M, Grivennikov SI, Guma M, Koltsova EK, Datz C *et al.* Fibroblast-specific protein 1 identifies an inflammatory subpopulation of macrophages in the liver. *Proc Natl Acad Sci USA* 2011; **108**: 308–313.
34 Cheng LH, Hung KF, Huang TF, Hsieh HP, Wang SY, Huang CY *et al.* Attenuation of cancer-initiating cells stemness properties by abrogating S100A4 calcium binding ability in head and neck cancers. *Oncotarget* 2016; **7**: 78946–78957.
35 Guo J, Bian Y, Wang Y, Chen L, Yu A, Sun X. S100A4 influences cancer stem cell-like properties of MGC803 gastric cancer cells by regulating GDF15 expression. *Int J Oncol* 2016; **49**: 559–568.
36 Atlasi Y, Noori R, Marolin I, Franken P, Brandao J, Biermann K *et al.* The role of S100a4 (Mts1) in Apc- and Smad4-driven tumour onset and progression. *Eur J Cancer* 2016; **68**: 114–124.
37 Cerezo LA, Remakova M, Tomcik M, Gay S, Neidhart M, Lukanidin E *et al.* The metastasis-associated protein S100A4 promotes the inflammatory response of mononuclear cells via the TLR4 signalling pathway in rheumatoid arthritis. *Rheumatology (Oxford)* 2014; **53**: 1520–1526.
38 Plestilova L, Mann H, Andres Cerezo L, Pecha O, Vencovsky J, Senolt L. The metastasis promoting protein S100A4 levels associate with disease activity rather than cancer development in patients with idiopathic inflammatory myopathies. *Arthritis Res Ther* 2014; **16**: 468.